Int. J. Nano Dimens., 7(4): 329-335, Autumn 2016

ORIGINAL ARTICLE

Electrical and optical properties of a small capped (5, 0) zigzag Carbon nanotube by B, N, Ge and Sn atoms: DFT theoretical calculation

Monir Kamalian[1, 3]; *Afshin Abbasi*[2,*]; *Yousef Seyed Jalili*[1,3]

[1]*Department of Physics, Science and Research Branch, Islamic Azad University, Tehran, Iran*
[2]*Department of Chemistry, University of Qom, Qom, Iran*
[3]*Nano-Optoelectronics Lab, Sheykh Bahaee Research Complex, Science and Research Branch, Islamic Azad University, Tehran, Iran*

Received 19 March 2016; revised 10 July 2016; accepted 03 August 2016; available online 28 December 2016

Abstract

In this study we investigate the effect of atoms such as B, N, Ge and Sn on the optical and the electrical properties of capped (5, 0) zigzag carbon nanotube, using DFT calculation method. These elements were attached to the one end of the carbon nanotube. We considered four different structure designs as possible candidates for a p-n junction device. The electrical properties of these structures were investigated using the quantum chemical information analysis which leads to the energy band gap, dipole moments, electrical charges and the DOS of these structures. Further TD-DFT calculations were performed to obtain the optical properties of the structure designs to investigate the electron mobility, indicating higher conductivity and higher rectifying voltage in the CNT terminated by Sn.

Keywords: *Ab inito calculation; Carbon nanotube; Electrical conductivity; p-n junction; TD-DFT calculation.*

How to cite this article

Kamalian M, Abbasi A, Seyed Jalili Y. Electrical and optical properties of a small capped (5, 0) zigzag Carbon nanotube by B, N, Ge and Sn atoms: DFT theoretical calculation. Int. J. Nano Dimens., 2016; 7 (4): 329-335, DOI: 10.7508/ijnd.2016.04.008.

INTRODUCTION

In recent years carbon nanotubes (CNTs) as well as other tubular nano materials have attracted considerable attention, among low-dimensional physical systems [1]. CNTs have significant potential for applications in molecular electronics [2, 3], nanomechanics [4], optics [5, 6], sensors [7-9] and also catalysis [10]. However, many applications, particularly in electronics and sensors, for improved device performance and its commercial success we have to control the device structural integrity at the molecular level. This is where *ab initio* calculations could play a crucial role in assessing and isolating various effects providing a useful guide-path to experimental fabrication. Indeed, much experimental development toward electronic devices based on carbon nanotubes has been reported [11-15]. In order to enrich the potential applications, the doping of other potential elements into Graphene nanostructures is the efficient way to fine tune the electronic structure properties leading to better device integrity and performance.

The p-n junction, which is characterized by rectification, is the main part of many devices in the semiconductor optoelectronics industry. Naturally, one of the main steps of development of CNTs based optoelectronic devices should be design and manufacture of CNT based *p-n* junction [16-18]. It is well known that N and B atoms, as neighbors of the C atom within the periodic Table, are generally considered as the accepted candidates for inclusion into carbon based nano-structures. Various techniques have been employed to incorporate N or B atoms into carbon nano-materials [19-21]. Alternatively, an atom by atom substitution technique using the scanning tunneling microscope could be realized to control nanostructures accurately. N/B dopant can inject electron/hole into carbon-based materials, thus changing their electronic and transport properties [22].

* Corresponding Author Email: *a.abbasi@qom.ac.ir*

Doping of Ge and Sn results in deformation and local polarization of perfect, have produced pure CNTs [23].

Ge nanostructures are of particular interest, since the exciton Bohr radius of bulk Ge is larger than that of other group-IV elements, resulting in more prominent quantum confinement effects in CNTs. Ge also offers the advantage of processing with easier integration into conventional devices. Furthermore, Ge has much higher electron and hole mobility than that of other group-IV elements, which is especially essential when electronic devices are scaled down to the order of 100 nm regime as in CNTs [24].

Using density functional theory (DFT) calculations, we have investigated the electronic structure, electrical and optical properties of B, N, Ge and Sn doped CNT structures with wide applications for technological purposes [25].

EXPERIMENTAL

Computational Methods

We have considered four CNT based design structures: An undoped CNT, as the reference, and three capped CNT models, illustrated in Fig. 1. For the undoped model (Fig. 1a) we have used a small (5, 0) Zigzag carbon nanotube containing in total 30 Carbon atoms. B/N doped CNT is illustrated in Fig. 1b, where B and N are connected to one end of the CNT, the region where the C atoms are more reactive. In this structure the terminal C atoms are replaced by B atoms.

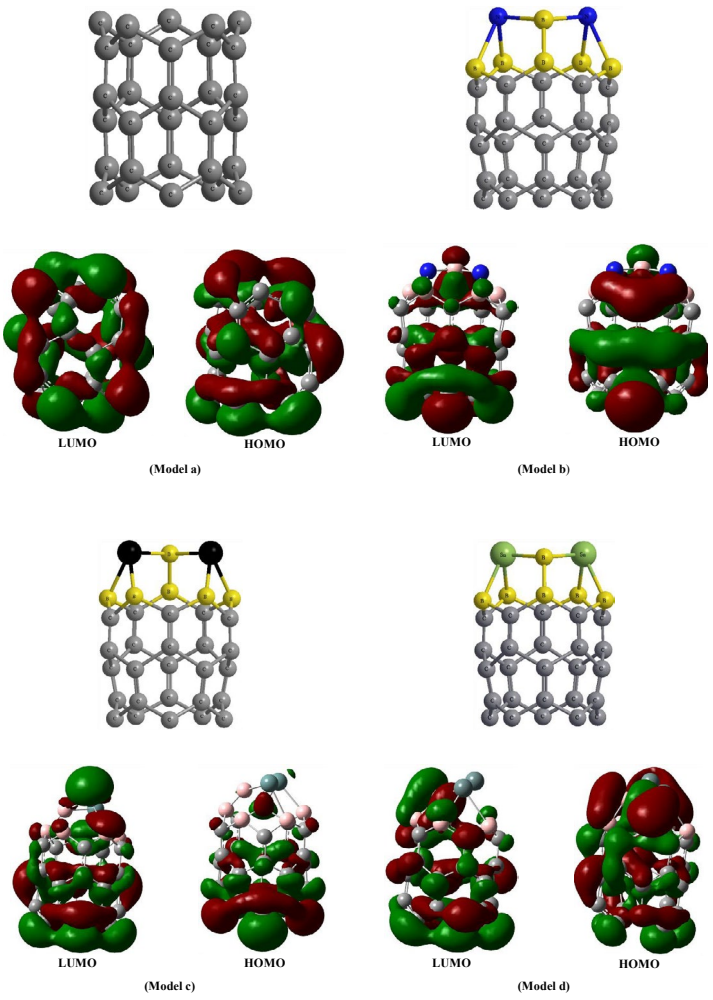

Fig. 1: The CNT structure models used in this study and their HOMO and LUMO orbitals. (a) Undoped (5, 0) carbon nanotube including 30 C atoms. (b) The structure of the pristine model in which one side was capped with B and N atoms. (c) The structure of the pristine model in which one side was capped with B and Ge atoms. (d) The structure of the pristine model with one side capped with B and Sn atoms.

The B atoms are connected to the C and two N atoms in its neighborhood. Fig. 1c and d illustrate structures in which the N atoms in model b are replaced by Ge atoms (model c) and with Sn atoms (model d) respectively. In the first step, the geometries of these structures were optimized using the Becke's hybrid three-parameter exchange functional and the nonlocal correlation functional of the Lee, Yang and Parr (B3LYP) method [26, 27] and the 6-311G(d) basis set in model a-c, and LanL2DZ basis set for model d were implemented in the Gaussian 03 [28] package.

RESULTS AND DISCUSSION

All the structures have been optimized at the theoretical levels discussed above and the optimized structures were used for further investigation.

HOMO-LUMO energy gap

The HOMO-LUMO gap is the energy gap between the lowest unoccupied molecular orbital (LUMO) and the highest occupied molecular orbital (HOMO). Table 1 presents the results for HOMO and LUMO energies, the HOMO-LUMO gaps and the dipole moments of design structures a-d obtained using DFT calculations.

From the data of Table 1, we can conclude that the design structures of models b and d have the lowest HOMO-LUMO energy gaps. Therefore these two structures can electrically be more conductive than the other structures considered. The HOMO-LUMO energy gap in structure c where Ge atoms have been icluded into the CNT is very approximately close to that of the pristine CNT (model a). Hence it could be concluded that Ge does not seem to be very effective in modifying the electrical conductivity of the CNT.

Analysis of Dipole Moments

Dipole moment acts as an additional scattering mechanism for the current carrying electrons which itself is the first derivative of the energy with respect to an external electric field. Many properties can be related directly to the dipole moments. The last column of Table 1 represents the dipole moments of the design structures, models a-d. It is interesting that the pristine model represents a relatively large dipole moment. The asymmetrically optimized structure of the pristine CNT (Fig. 1a) is the reason of the unacceptable computed dipole moment. Substitution of Sn and Ge at the N sites raises the dipole moment of structures c and d. The relatively larger atomic size of Sn is the reason of the highest dipole moment (5.55 Debye) observed in the design structure model d.

Density of states (DOS)

In molecules, the possible electronic energies are discrete, quantized energy levels. As molecules become larger, these energy levels move closer together. One important question is how many orbitals are available at any given energy level. This can be shown and investigated by using the DOS spectra calculations. The band structure and DOS provide adequate information regarding the conductivity of the CNT structures as well as more complex geometric and electronic configurations. A material with a half-filled energy band is a conductor, but it may be a very poor conductor if there are very few unfilled orbitals available close to the frontier orbitals (chemical potential).

Fig. 2 illustrates the DOS of the CNT models calculated using the Gauss Sum 3.0 [29] Program package. This package reads the output eigenvalues from the Gaussian 03 output file. The figures indicate that by including dopant atoms of B, N, Ge and Sn, it is possible to strongly modify the DOS of the Pristine CNT (model a). This modification is most prominent in the last two models c and d, in which the density of the frontier unoccupied molecular orbitals has dominantly increased.

Table 1: E_{HOMO}, E_{LUMO}, HOMO-LUMO energy gap $_{(\Delta(LUMO\text{-}HOMO))}$ total NBO charges on the C atoms and dopand atoms and the dipole moments for models a–c calculated using B3LYP method.

Models	E_{LUMO} (ev)	E_{HOMO} (ev)	$\Delta_{(LUMO\text{-}HOMO)}$ (ev)	Total Charge on C atoms	Total Charge on non-C atoms	Dipole Moment (Debye)
(a) Pristine	-3.90	-5.30	1.40			1.68
(b) CNT B-N	-4.89	-6.11	1.22	-2.6	+2.6	2.34
(c) CNT Ge-B	-4.24	-5.70	1.46	-3.0	+3.0	2.46
(d) CNT Sn-B	-4.58	-5.79	1.21	-3.5	+3.5	5.55

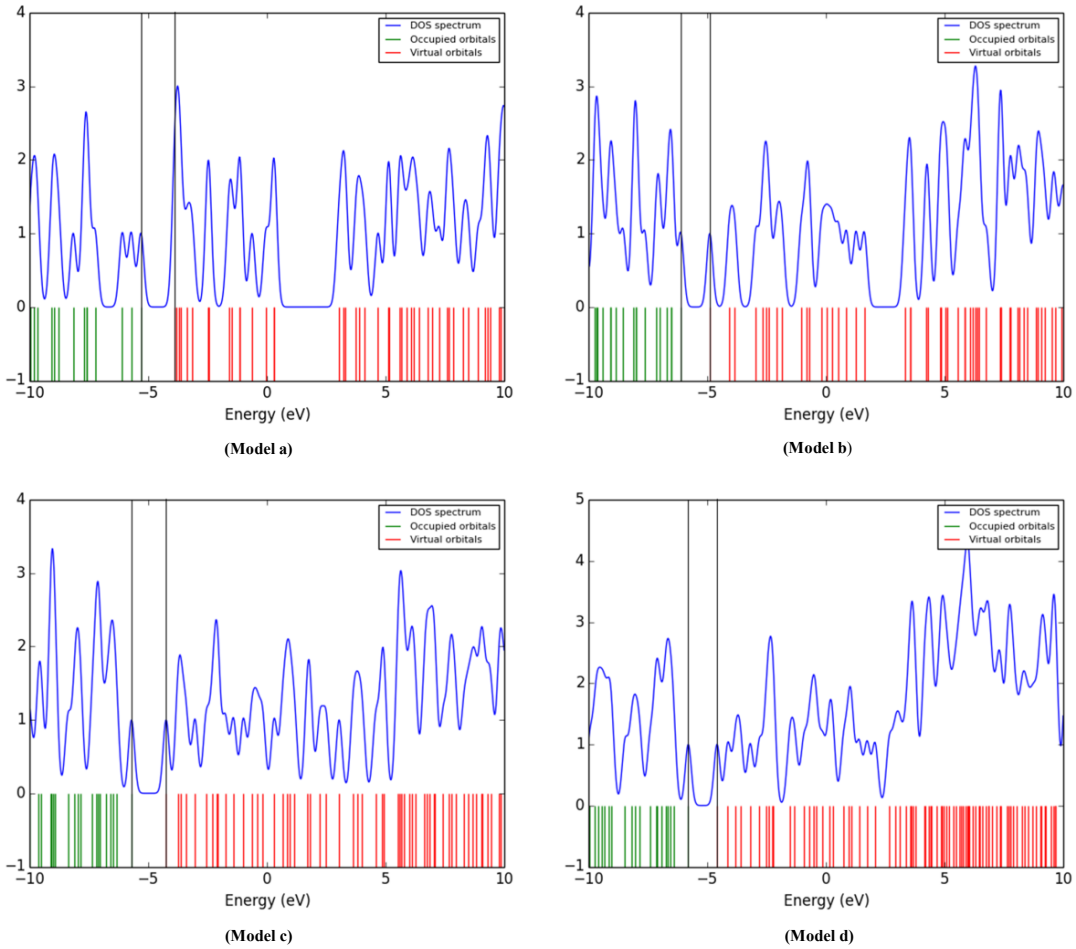

Fig. 2: Density of state versus energy for models a-d (The energy gaps are indicated by parallel black lines). Blue lines represent the DOS spectrum, green and red lines represent occupied and unoccupied orbitals respectively.

Electrical charge analysis

The population analysis has been performed to determine the local charge distributions of atoms using the natural bond orbital (NBO) [30] analysis and B3LYP method of calculations. We assumed each structure is divided in two parts concerning the localized charges on atoms (except the pristine model). The carbon part which included the total charge of all the carbon atoms and the non-carbon atoms side has included the total charge of all the other atoms. The total charge of each part (Table 1) indicates that the carbon atoms holding the negative charges represent the n-side, and the non-carbon atoms holding the positive charges, represent the p-side of a p-n junction. The high negative and positive localized charges on both sides represent electrical current rectifying effect in the p-n junction which could be fabricated from these CNT based design structures. The higher localized charge reveals the potential ability of a higher rectifying voltage in a p-n junction, the rectifying voltage increases from the design structure b to structure d.

Optical absorptions

In optoelectronic industry, it is crucial to investigate the characteristic of the light absorption and emission spectra. To determine this absorption theoretically, Time-Dependent Density Functional Theory (TD-DFT) was used. The TD-DFT calculations were implemented using the B3LYP method and the 6-31G(d,p) basis sets for models a-c and LanL2DZ basis sets for model d. To represent the absorption spectra graphically the Gaussian software TD-DFT calculated results were converted to Gaussian functions using Gauss Sum 3.0. To produce realistic looking spectra the full width at half maximum of the Gaussian

functions was set at 3000 cm^{-1}. Fig. 3 depicts the absorption spectra of the pristine and the doped CNT structures. The observed differences in the absorption spectra indicate that the electronic structure of the CNTs are strongly modified by the dopant atoms incorporated into the pristine CNT resulting in the disruption of the aromatic system of the undoped pristine CNT, which in turn causes changes in the conductivity. TD-DFT calculations (Fig. 3) show that the optical absorption are all within the wavelength range proximity of near infrared (NIR) spectra.

Therefore if these materials are to be used in optoelectronic they will not be suitable for visible device applications. Instead, for the NIR optoelectronic industry there mays be considerable potential applications.From the oscillator strengths and coefficients of the wave functions of transition represented in Table 2 it could be seen that for the pristine model the absorption peak occurs at the wavelength of 1482 nm from the excitation of HOMO to LUMO+1, in model b the peak absorption is at 1182 nm from HOMO-2 to LUMO, and in the structure c the peak absorption is at 1240 nm from HOMO to LUMO. In model d the peak absorption occurs at 1043 nm from HOMO to LUMO+1. From the gap between the HOMO and LUMO of these structures we have concluded that structures b and d have lower gap and higher conductivity compared to pristine CNT. The density of states in Fig. 2 represent the gap between the LUMO and LUMO+1 in the conduction band in two models of d and b. Therefore an excited electron to the LUMO is not able to further conduct in the conduction band where the thermal energy maybe not enough to excite this electron to the higher unoccupied MOs. As the structure d represents a strong absorption to the LUMO+1 therefore in this structure the absorption of the light can carry electron through the molecule.

From these results alongside the arguments discussed, it could be concluded that the model d has considerably better electrical properties i.e. better conduction properties.

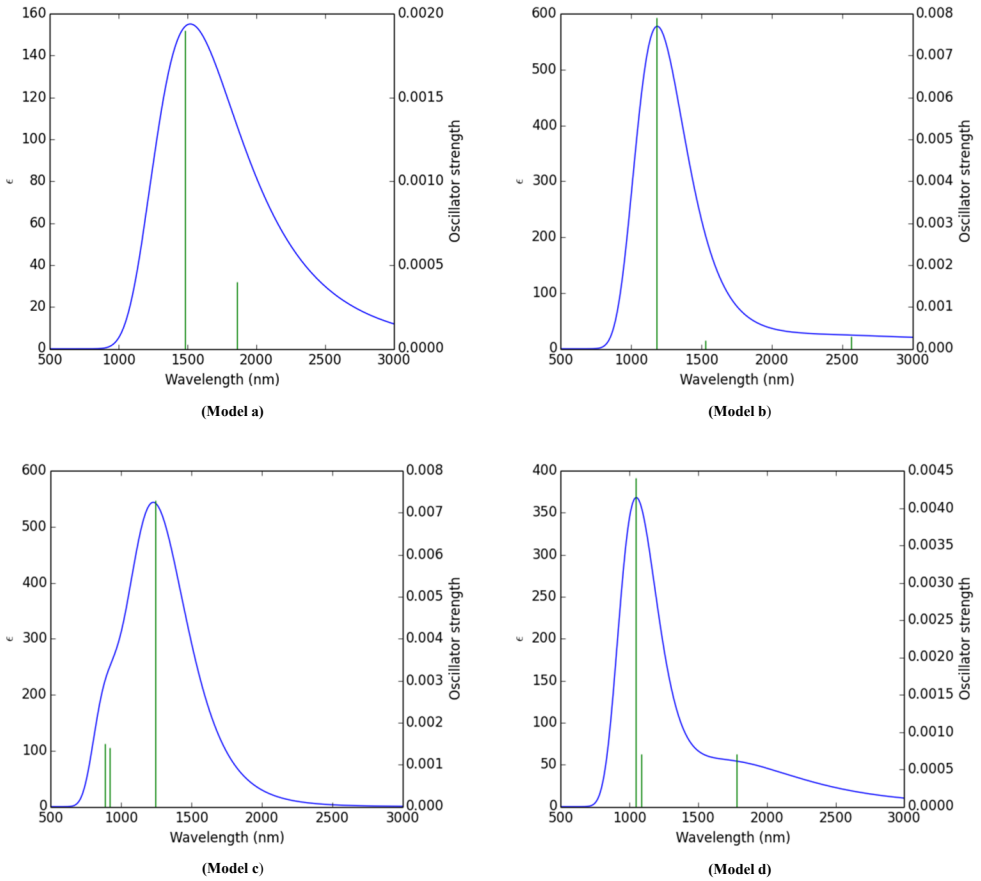

Fig. 3: TD-DFT calculated electronic absorption spectra of the models a-d illustrated in Fig. 1.

Table 2: Theoretical wavelengths (in nm) and contribution of major orbitals in the absorption spectra.

Model	Absorption wavelength (nm)	Orbital involved	Oscillation strength	Major contributions
Model a	1860	HOMO→LUMO	0.0004	0.91
		HOMO→LUMO+3		0.06
	1482	HOMO→LUMO+2	0.0019	0.97
Model b	2561	HOMO→LUMO	0.0003	1
	1526	HOMO-1→LUMO	0.0002	0.99
	1182	HOMO-2→LUMO	0.0079	0.92
		HOMO-3→LUMO		0.9
Model c	1240	HOMO→LUMO	0.0073	0.95
		HOMO-1→LUMO		0.03
	921	HOMO→LUMO+1	0.0014	0.37
		HOMO→LUMO+2		0.52
		HOMO-1→LUMO		0.03
		HOMO→LUMO		0.02
		HOMO→LUMO+4		0.02
	886	HOMO-1→LUMO	0.0015	0.34
		HOMO→LUMO+1		0.43
		HOMO→LUMO+2		0.15
		HOMO-2→LUMO		0.03
Model d	1779	HOMO→LUMO	0.0007	0.98
	1087	HOMO-1→LUMO	0.0007	0.75
		HOMO→LUMO+1		0.13
		HOMO-5→LUMO		0.02
		HOMO-3→LUMO		0.03
		HOMO-2→LUMO		0.04
	1043	HOMO-2→LUMO	0.0044	0.18
		HOMO→LUMO+1		0.72
		HOMO-4→LUMO		0.03
		HOMO-1→LUMO		0.05

CONCLUSION

In this work, DFT calculations were used to investigate and compare the optical, electrical and chemical properties of a small (5, 0) pristine zigzag carbon nanotube and three other doped structures of the carbon nanotube, which were capped by B/N, Ge and Sn atoms. The geometries of these structures were optimized at the B3LYP level using 6-311G(d) and LanL2DZ basis sets. Dipole moments, HOMO-LUMO energy gaps, Density of states (DOS), UV/Vis spectrums, oscillator strengths (*f*) and the coefficients of the wave functions corresponding to the particular transitions of these structures have been comparatively investigated. According to the calculated dipole moments for the CNT models, due to the large atomic size of Sn, higher value of dipole moment was observed for the carbon nanotube which was terminated by Sn atoms.

The calculation of the DOS spectrum provided important information on the conduction properties of the structures. TD-DFT calculations were used to investigate the UV/Vis spectrums. Due to the higher density of states, smaller band gap and the strong frequency absorption to the LUMO+1 in the structure containing Sn atoms, we deduced that Sn element is the best choice among B, N, Sn and Ge used in this study according to the electron mobility improvement. The developed conclusions presented were based on the optical and electrical properties that were obtained from the quantum chemical calculations in order to reach a qualitative comparative study.

CONFLICT OF INTEREST

The authors declare that there is no conflict of interests regarding the publication of this manuscript.

REFERENCES

[1] Mceuen P. L., Fuhrer M. S., Park H., (2002), Single-walled carbon nanotube electronics. *IEEE Trans. Nanotechnol.* 1: 78-85.

[2] Lugli P., Di Carlo A., (2004), Molecular electronics. 4th IEEE conference on *Nanotechnology.* (Tutorial 3).

[3] Yam Ch., Mo Y., Wang F., Li X., Chen G., Zheng X., (2008), Dynamic admittance of carbon nanotube-based molecular electronic devices and their equivalent electric circuit. *Nanotehnol.* 19: 495203-495300.

[4] Srivastava D., Wei Ch., Cho K., (2003), Nanomechanics of carbon nanotubes and composites. *Appl. Mech. Rev.* 56: 215-230.

[5] Avouris Ph., Freitag M., Perebeinos V., (2008), Carbon-nanotube photonics and optoelectronics. *Nature photonics.* 2: 341-350.

[6] Rida J., Bahardiwaj A. K., Jaiswal A. K., (2014), Design optimization of optical communication systems using carbon nanotubes (CNTs) based on optical code division multiple access (OCDMA). *Int. J. Comp. Sci. Network Security*. 14: 102-112.

[7] Zhukovskii Y., Piskunov S., Pungo N., Berzina B., (2009), Ab initio simulations on the atomic and electronic structure of single-walled BN nanotubes and nanoarches. *J. Phys. Chem. Solids.* 70: 796-803.

[8] Niraj S., Jiazhi M., John T. W. Y., (2006), carbon nanotubes based sensors. *J. Nanosci. Nanotech.* 18: 573-590.

[9] Peng Sh., O`Keefe J., Wei Ch., Cho K., (2001), Carbon nanotubes chemical and mechanical sensors. *Conference paper for the 3th International Workshop on structural health monitoring*.

[10] Yan Y., Miao J., Yang Zh., Xing-Xiao F., Bin Yang H., Lio B., (2015), Carbon nanotube catalysts: recent advances in synthesis, characterization and applications. *Chem. Soc. Rev.* 44: 3295-3346.

[11] Javey A., Guo J., Wang Q., Lundstrom M., Dai H., (2003), Ballistic carbon nanotube field-effect transistors. *Nature*. 424: 654-657.

[12] Mann D., Javey A., Kong J., Wang Q., Dai H., (2003), Ballistic transport in metallic nanotubes with reliable Pd ohmic contacts. *Nano Lett.* 3: 1541-1544.

[13] ScarSelli M., Castrucci P., De Crescenzi M., (2012), Electronic and optoelectronic nano-devices based on carbon nanotubes. *J. Phys. Condens. Matter.* 24: 313202-313238.

[14] Rosenblatt S., Yaish Y., Park J., Gore J., Sazonova V., (2002), High performance electrolyte gated carbon nanotube transistors. *Nano Lett.* 2: 869-872.

[15] Seidel R. V., Graham A. P., Kretz J., Rajasekharan B., (2005), Sub-20 nm short channel carbon nanotube transistors. *Nano Lett.* 5: 147-150.

[16] Pecchia A., Carlo A. Di, (2004), Atomistic theory of transport in organic and inorganic nanostructures. *Rep. Prog. Phys.* 67: 1497-1561.

[17] Kamalian M., Jalili Y. S., Abbasi A., (2015), Density functional theory of the carbon nanotube based p-n junction by substitutation of carbon atoms with B, N, Ge and Sn. *Indian J. Phys.* 89: 663-669.

[18] Najafpour J., Monajjemi M., Aghaei H., Zare K., (2015), The chemical electronic properties of PNP molecular transistor based on (4, 3) chiral. *Fuller. Nanotub. Car. N.* 23: 218-232.

[19] Czerw R., Terrones M., Charlier J. C., Blasé X., Foley B., (2001), Identification of electron donor states in N-doped carbon nanotubes. *Nano lett.* 1: 457-460.

[20] Li J., Glerup M., Khlobystov A. N., Wiltshire J. N., (2006), The effects of nitrogen and boron doping on the optical emission and diameters of single-walled carbon nanotubes. *Carbon*. 44: 2752-2757.

[21] Wei D. C., Liu Y. Q., Wang Y., Zhang H., Huang L., Yu J., (2009), Synthesis of N-doped graphene by chemical vapor deposition and its electrical properties. *Nano Lett.* 9: 1752-1758.

[22] Yu S. S., Zheng W. T., (2010), Effect of N/B doping on the electronic and field emission properties for carbon nanotubes, carbon nanocones and graphene nanoribbons. *Nanoscale*. 2: 1069-1082.

[23] Chakraborty B., Modak P., Banerjee S., (2010), Deformation and polarization in single walled carbon nanotube due to doping of group-IV elements: A principle investigation. *AIP Conf. Proc.* 1313: 364-367.

[24] Qian D., Crocker M., Pandurangan A., Morin C., (2010), Synthesis of germanium/multi-walled carbon nanotube coresheath structures via chemical vapor deposition. Croatia, DC*: Intech*.

[25] Hierold C., Jungen A., Stampfer C., Helbling T., (2007), Nano electromechanical sensors based on carbon nanotubes. *Sensors and Actuators A-Physical.* 136: 51-61.

[26] Becke A. D. J., (1993), Density-functional thermochemistry. III. The role of exact exchange. *Chem. Phys.* 98: 5648-5653.

[27] Lee C., Yang W., Parr R. G., (1998), Development of the colle-salvetti correlation energy formula into a functional of the electron density. *Phys. Rev. B.* 37: 785-790.

[28] Frisch M. J., Trucks J. W., Schlegel H. B., Scuseria G. E., Rob M. A., Cheeseman J. R., (2009), *Gaussian 03* (Revision Gaussian), Inc., Wallingford, CT.

[29] O'Boyle N., (2013), *GaussSum 3.0*, GaussSum Inc., (Cambridge, UK).

[30] Reed A. E., Curtiss L. A., Weinhold F., (1988), Intermolecular interaction from a natural bond orbital, donor-acceptor viewpoint. *Chem. Rev.* 88: 899-926.